

MHD boundary layer flow due to an exponentially stretching surface through porous medium with radiation effect



Faisal Salah*, Ahmad Almohammadi

Department of Mathematics, College of Science and Arts, Rabigh, King Abdul-Aziz University, Jeddah, Saudi Arabia

ARTICLE INFO

Article history:

Received 8 May 2023

Received in revised form

5 October 2023

Accepted 3 November 2023

Keywords:

Second-grade fluid

MHD

Heat transfer

ABSTRACT

The purpose of this article is to study the boundary layer flow and heat transfer of the MHD second-grade fluid. By utilizing similarity transformations, the governing equations are transformed into a set of non-linear ordinary differential equations. To get semi-analytical formulations of velocity, temperature, and other variables, we use the homotopy analysis technique (HAM). Then, we employ the Wolfram Language function NSolve to get the solutions. The main finding of the present work is that the flow variables have been influenced by the magnetic field parameter, the porous parameter, and the radiation parameter.

© 2023 The Authors. Published by IASE. This is an open access article under the CC BY-NC-ND license (<http://creativecommons.org/licenses/by-nc-nd/4.0/>).

1. Introduction

Numerous industries use heat transfer in their daily operations. In engineering and industrial operations, the creation of materials with high thermal conductivity and a quick rate of heat movement is crucial. Heat transfer in non-Newtonian fluids has attracted a lot of attention due to its numerous industrial, electronic, and biomedical applications. To examine the heat transfer in the boundary layer adjacent to a vertical plate, Nakayama and Koyama (1987) have found a similarity solution. A nonsimilar solution for combined convection boundary layer flow adjacent to a vertical plate with variable surface temperature has been discussed by Hsieh et al. (1993). Pal (2010) investigated the MHD non-Darcy mixed convection heat transfer from a vertical heated plate. He found that the magnetic field significantly affects both the velocity of the boundary layer and the rate of heat transfer. There is a huge number of papers on this subject we refer the reader to read (Kalpana et al., 2022; Kausar et al., 2022; Roy and Pop, 2020; Khashi'ie et al., 2022; Zainal et al., 2021) and references therein. The boundary layer has attracted the attention of scientists and researchers due to its numerous uses in a variety of industrial, manufacturing, biomedical, and engineering

phenomena. Boundary layer theory has been effectively applied to Newtonian and non-Newtonian fluids during the past decades (Chhabra and Richardson, 1999). The non-Newtonian models are vastly used in the literature. Simply because the non-Newtonian models have real applications in a variety of engineering applications. One of the most important non-Newtonian models is the second-grade fluid. The second-grade fluid is frequently cited in the literature because it has numerous applications in the fields of bioengineering, food processing, drilling, and metallurgy (Trüedell and Noll, 1965). There are numerous investigations that discussed the second-grade fluid through the boundary layer (Vajravelu and Roper, 1999; Hayat et al., 2008; Roy and Pop, 2020; Shah et al., 2022; Khan et al., 2022). Due to its advantages in the fields of engineering and technology application, the study of magneto hydrodynamics (MHD) boundary layer flow has attracted a lot of attention recently. Liquid metal cooling blankets for fusion reactors, the metallurgical process, and the stretching of plastic sheets are just a few examples of the MHD's numerous uses Kefayati (2016) and Daniel et al. (2017). Emam and Elmaboud (2017) studied the 3D MHD boundary layer flow with heat transfer. They found that the nanoparticle volume fraction and magnetic field strength play a role in the variation of both the fluid temperature and velocity. The influences of the Lorentz force and buoyancy in iron oxide-water nanofluid within a porous cavity have been investigated by Sheikholeslami (2019a). Urgorri et al. (2021) investigated the impact of MHD boundary layers on tritium permeation in PbLi flows for fusion breeding blankets. Liu et al. (2020) discussed the magnetic effect on the Sobolev

* Corresponding Author.

Email Address: frashed@kau.edu.sa (F. Salah)<https://doi.org/10.21833/ijaas.2023.11.020>

Corresponding author's ORCID profile:

<https://orcid.org/0000-0003-0410-001X>

2313-626X/© 2023 The Authors. Published by IASE.

This is an open access article under the CC BY-NC-ND license

<http://creativecommons.org/licenses/by-nc-nd/4.0/>

solvability of boundary layer equations for the 2D incompressible MHD. Recently, Reddy et al. (2022) investigated the impacts of the rotation and diffusion-thermo on time-dependent heat-generated MHD chemically reactive mixed-convection Casson fluid. They employed the finite element method to get the numerical solution of the governing boundary layer equations. Sheikholeslami (2018) used the CVFEM to examine the influence of variable magnetic field on nanofluid and heat transfer in a cavity. He found that the Lorentz forces cause the nanofluid motion to decrease and augment the thermal boundary layer thickness. A novel computational technique for the consideration of the effect of magnetic forces on ferro fluid has been described by Sheikholeslami (2019a). Results show that a reduction in magnetic force causes an exergy decline. Sheikholeslami (2019b) discussed a numerical approach to demonstrate nanofluid MHD flow through a porous enclosure. The roles of the radiation parameter and the Hartmann and Rayleigh numbers are also discussed.

In light of the reviews mentioned above, the current study focuses on getting the semi-analytical solutions for the MHD boundary layer flow and heat transfer of the second-grade fluid. The problem is formulated and transformed into a system of non-linear ODEs using the similarity transformation. The semi-analytical solution via the homotopy analysis method (HAM) will be applied. For the validity of the solutions, we will compare the results with the numerical results obtained by Bidin and Nazar (2009). The physical features of embedding parameters are discussed through graphs.

2. Formulation of problem

Consider a steady, incompressible, electrically conducting MHD second-grade fluid flow through a porous medium adjacent to a vertical surface (Fig. 1). It is assumed that a consistent magnetic field of intensity B is applied in the positive-direction, normal to the surface. The system of equations that

models the boundary layer flow through a porous medium along the Boussinesq approximations is as follows:

$$\frac{\partial U}{\partial X} + \frac{\partial V}{\partial Y} = 0, \tag{1}$$

$$U \frac{\partial U}{\partial X} + V \frac{\partial U}{\partial Y} = \nu \frac{\partial^2 U}{\partial Y^2} + \gamma \left(U \frac{\partial^3 U}{\partial X \partial Y^2} + \frac{\partial U}{\partial X} \frac{\partial^2 U}{\partial Y^2} + V \frac{\partial^3 U}{\partial Y^3} + \frac{\partial U}{\partial Y} \frac{\partial^2 U}{\partial Y^2} \right) - \left(-\frac{\sigma B^2}{\rho} + \frac{\nu}{k} \right) U, \tag{2}$$

$$U \frac{\partial T}{\partial X} + V \frac{\partial T}{\partial Y} = \frac{k}{c_p} \frac{\partial^2 T}{\partial Y^2} - \frac{1}{c_p} \frac{\partial q_r}{\partial y}, \tag{3}$$

where, $B = B_0 e^{\frac{X}{2L}}$, $q_r = -\frac{4\sigma^*}{3k^*} \frac{\partial T^4}{\partial Y}$, σ^* is the Stefan-Boltzmann constant, k^* is the absorption coefficient. Through Taylor's series, we can write $T^4 = 4T_\infty^3 T - 3T_\infty^4$. The appreciated boundary conditions are:

$$U = U_w = U_0 e^{\frac{X}{2L}}, V = 0, T = T_w = T_\infty + T_0 e^{\frac{X}{2L}} \text{ at } Y = 0, \\ U \rightarrow 0, T \rightarrow T_\infty, \text{ as } Y \rightarrow \infty, \tag{4}$$

where, (U, V) are the velocities in (X, Y) -directions, ν is the kinematic viscosity, γ is the viscoelastic parameter, σ is the electrical conductivity, density, T is the fluid temperature, k is the thermal conductivity, C_p represents heat capacitance, q_r is the radiative heat flux and U_w the mass transfer velocity at the surface. Introducing the non-dimensional variables as follows:

$$\xi = \sqrt{\frac{U_0}{2\nu L}} e^{\frac{X}{2L}} Y, U = U_0 e^{\frac{X}{2L}} g'(\xi), \\ V = -\sqrt{\frac{\nu U_0}{2L}} e^{\frac{X}{2L}} [g(\xi) + \xi g'(\xi)], T = T_\infty + T_0 e^{\frac{X}{2L}} \vartheta, \tag{5}$$

where, T_w is the variable temperature at the surface. Substituting the non-dimensional variables (Eq. 5) into Eqs. 1-3. The equations will be reduced to the following system of non-linear ODEs as follows:

$$2g'^2 - gg'' = g''' + \lambda \left[g'g''' - \frac{1}{2}gg'''' - \frac{3}{2}g''^2 \right] - 2(M + Da)g', \tag{6}$$

$$\left(1 + \frac{4}{3}\beta \right) \vartheta'' + Pr[g\vartheta' - g'\vartheta] = 0 \tag{7}$$

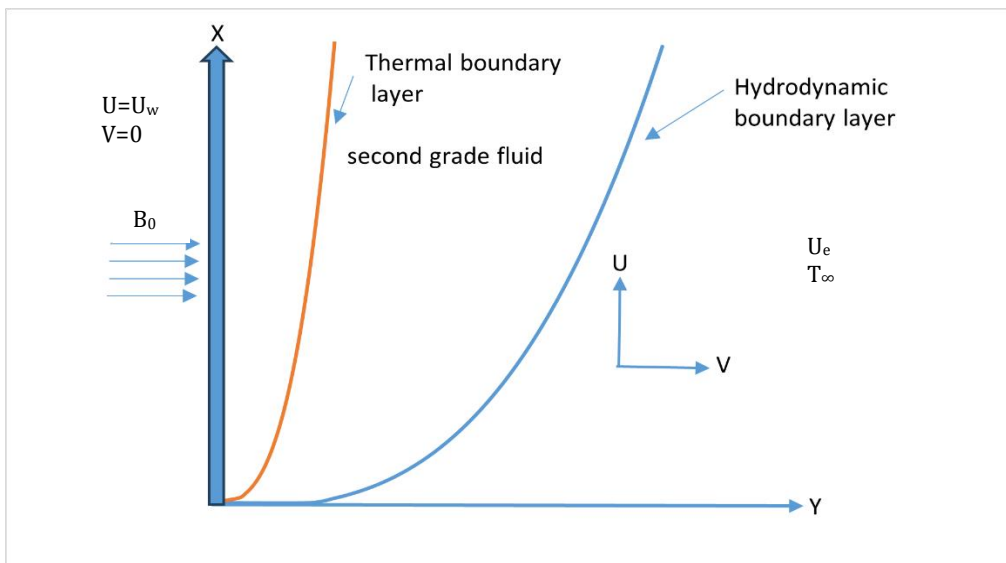


Fig. 1: Geometrical configuration

The non-dimensional boundary conditions will be:

$$g' = 1, g = 0, \vartheta = 1, \quad \text{at } \xi = 0, \\ g' \rightarrow 0, g'' \rightarrow 0, \vartheta \rightarrow 0, \text{ as } \xi \rightarrow \infty, \quad (8)$$

where, $\lambda = \frac{\gamma U_0}{\nu L} e^{\frac{X}{L}}$ is the viscoelastic parameter, $M = \frac{\sigma B_0^2}{A}$ is the magnetic parameter, $Da = \frac{\nu L}{K U_0} e^{-\frac{X}{L}}$ is the porous parameter, $\beta = \frac{4\sigma^* T_\infty^3}{k k^*}$ is the radiation parameter, and $Pr = \frac{\nu C_p}{k}$ is the Prandtl number.

The skin friction coefficient C_f , and the local Nusselt number Nu_x are defined as:

$$C_f = \frac{\tau_w}{\rho U_0^2} e^{\frac{2X}{L}}, Nu_x = \frac{L Q_w}{k(T_w - T_\infty)}, \quad (9)$$

where, τ_w , and Q_w are the wall shear stress and heat flux, and they are defined as:

$$\tau_w = \nu \frac{\partial U}{\partial Y} \Big|_Y = 0 + \gamma(U \frac{\partial^2 U}{\partial X \partial Y} + 2 \frac{\partial U}{\partial X} \frac{\partial U}{\partial Y} + V \frac{\partial^2 U}{\partial Y^2}) \Big|_Y = 0, \\ Q_w = (-k \frac{\partial T}{\partial Y} + q_r) \Big|_Y = 0, \quad (10)$$

using Eq. 5, Eq. 9, and Eq. 10, we found:

$$(2Re)^{\frac{1}{2}} C_f = (1 + \frac{3}{2} \lambda) g''(0), \quad \sqrt{2} Re^{-\frac{1}{2}} Nu = -(1 + \frac{4}{3} \beta) \vartheta'(0), \quad (11)$$

where, $Re = (\frac{U_0 L}{\nu}) e^{\frac{X}{L}}$ is the Reynolds number. The analytical solution of Eq. 6 when $M = Da = 0$, is:

$$g(\xi) = \sqrt{1 + \lambda} (1 - e^{-\frac{\xi}{\sqrt{1 + \lambda}}}). \quad (12)$$

2.1. The HAM solution to the problem

For HAM solutions of the governing Eqs. 6 and 7, we choose the initial approximations of g and ϑ (satisfy the boundary conditions) as follows:

$$g_0 = 1 - \exp[-\xi] \quad (13)$$

$$\vartheta_0 = \exp[-\xi] \quad (14)$$

and the auxiliary linear operators are $L_1(g) = \frac{\partial^3 g}{\partial \xi^3} - \frac{\partial g}{\partial \xi}$ and $L_2(\vartheta) = \frac{\partial^2 \vartheta}{\partial \xi^2} + \frac{\partial \vartheta}{\partial \xi}$. These auxiliary linear operators satisfy the following:

$$L_1(c_1 \exp[\xi] + c_2 \exp[-\xi] + c_3) = 0, \quad (15)$$

$$L_2(c_4 + c_5 \exp[-\xi]) = 0, \quad (16)$$

where, c_1, c_2, c_3, c_4, c_5 are constants. Introducing a non-zero auxiliary parameter \hbar , we develop the zeroth-order deformation problems as follows:

$$(1 - p)[L_1(g(\xi; p)) - L_1(g_0(\xi))] = \hbar p N(g(\xi; p)), \quad (17)$$

$$(1 - p)[L_2(\vartheta(\xi; p)) - L_2(\vartheta_0(\xi))] = \hbar p N(\vartheta(\xi; p)), \quad (18)$$

with the boundary conditions

$$g(\xi; p) = 0, \frac{\partial g(\xi; p)}{\partial \xi} = 1, \vartheta(\xi; p) = 1 \text{ at } \xi = 0, \quad (19)$$

$$\frac{\partial g(\xi; p)}{\partial \xi} \Rightarrow 0, \vartheta(\xi; p) \Rightarrow 0 \text{ as } \xi \Rightarrow \infty.$$

where, nonlinear operators, $L_1(g(\xi; p))$ and $L_2(\vartheta(\xi; p))$ are defined as:

$$L_1(g(\xi; p)) = \frac{\partial^3 g(\xi; p)}{\partial \xi^3} - 2 \frac{\partial g(\xi; p)}{\partial \xi} \frac{\partial g(\xi; p)}{\partial \xi} + g(\xi; p) \frac{\partial^2 g(\xi; p)}{\partial \xi^2} \quad (20)$$

$$+ \lambda [\frac{\partial g(\xi; p)}{\partial \xi} \frac{\partial^3 g(\xi; p)}{\partial \xi^3} - \frac{1}{2} g(\xi; p) \frac{\partial^4 g(\xi; p)}{\partial \xi^4} - \frac{3}{2} \frac{\partial^2 g(\xi; p)}{\partial \xi^2}] - 2(M + Da) \frac{\partial g(\xi; p)}{\partial \xi},$$

$$L_2(\vartheta(\xi; p)) = (1 + \frac{4}{3} \beta) \frac{\partial^2 \vartheta(\xi; p)}{\partial \xi^2} + Pr [g(\xi; p) \frac{\partial g(\xi; p)}{\partial \xi} - \frac{\partial g(\xi; p)}{\partial \xi} \vartheta(\xi; p)]. \quad (21)$$

When p increases from 0 to 1, $g(\xi; p)$ and $\vartheta(\xi; p)$ vary from $g_0(\xi)$ and $\vartheta_0(\xi; p)$ to $g(\xi)$, and $\vartheta(\xi)$ respectively. Using Taylor's theorem $g(\xi; p)$ and $\vartheta(\xi; p)$ can be expanded in a power series of p as follows:

$$g(\xi; p) = g_0(\xi) + \sum_{m=1}^{\infty} p^m g_m(\xi), \quad (22)$$

$$\vartheta(\xi; p) = \vartheta_0(\xi) + \sum_{m=1}^{\infty} p^m \vartheta_m(\xi), \quad (23)$$

where,

$$g_m(\xi; p) = g_m(\xi) = \frac{1}{m!} \frac{\partial^m g(\xi; p)}{\partial p^m} \text{ and } \vartheta_m(\xi) = \frac{1}{m!} \frac{\partial^m \vartheta(\xi; p)}{\partial p^m} \quad (24)$$

a non-zero auxiliary parameter \hbar is chosen in such a way that the series (Eq. 22 and Eq. 23) are convergent at $p = 1$. Suppose that the auxiliary parameter \hbar is selected such that the series (Eq. 22 and Eq. 23) are convergent at $p = 1$, then we have:

$$g(\xi) = g_0(\xi) + \sum_{m=1}^{\infty} g_m(\xi), \quad (25)$$

$$\vartheta(\xi) = \vartheta_0(\xi) + \sum_{m=1}^{\infty} \vartheta_m(\xi). \quad (26)$$

Differentiating the zeroth-order deformation Eqs. 17 and 18, m times with respect to P and then dividing them by $m!$ and finally setting $p = 0$, we have the following m th-order deformation problem:

$$L_1[g_m(\xi) - \chi_m g_{m-1}(\xi)] = \hbar R_m^g(\xi), \quad (27)$$

$$L_2[\vartheta_m(\xi) - \chi_m \vartheta_{m-1}(\xi)] = \hbar R_m^\vartheta(\xi). \quad (28)$$

Where, the recurrence formulae are,

$$= g_{m-1}''' + \sum_{i=0}^{m-1} (-2g'_{m-1-i} g'_i + g_{m-1-i} g''_i + \lambda [g'_{m-1-i} g'''_i - \frac{1}{2} g_{m-1-i} g''''_i - \frac{3}{2} g''_{m-1-i} g''_i]) \\ R_m^g(\xi) - 2(M + Da) g'_{m-1}, \quad (29)$$

$$R_m^\vartheta = (1 + \frac{4}{3} \beta) \vartheta''_{m-1} + Pr \sum_{i=0}^{m-1} [g_{m-1-i} \vartheta'_i - g'_{m-1-i} \vartheta_i]. \quad (30)$$

where,

$$\chi_m = \begin{cases} 0, & m \leq 1 \\ 1, & m > 1 \end{cases} \quad (31)$$

with the boundary conditions

$$g_m = 0, g'_m = 0, \vartheta_m = 0 \text{ at } \xi = 0, \\ g'_m \Rightarrow \vartheta_m \Rightarrow 0 \text{ as } \xi = \infty. \quad (32)$$

We use MATHEMATICA software to obtain the solution of these equations. The solutions will depend on the auxiliary parameter \hbar , which gives the convergence region and rate of approximation for the homotopy analysis method. To determine this parameter, we used the optimal method. In order to ensure the accuracy of our method, some obtained HAM results of the wall temperature gradient $-\vartheta(0)$ for different values of Pr and β keeping $M = Da = 0$ are given in Table 1 and compared with the numerical results obtained by Bidin and Nazar (2009). It can be seen that these results are in very good agreement. Moreover, at $\lambda = M = Da = 0$, we

found $-g''(0) = 1.281832$ after the tenth iteration, which is in good agreement with $f''(0) = 1.28181$ and $f''(0) = 1.28180$ reported in Bidin and Nazar (2009) and Elbashbeshy (2001), respectively. The influences of the viscoelastic parameter λ , the magnetic parameter M , and the porous parameter Da on the amount of the skin friction coefficient $|C_f|$ is shown in Table 2. We can conclude that the skin friction coefficient increases by increasing the viscoelastic parameter, the magnetic parameter and the porous parameter.

Table 1: Values of $-\vartheta(0)$ in the Newtonian fluid for various values of Pr when $M = Da = 0$

β	Bidin and Nazar (2009)			HAM		
	$Pr = 1$	$Pr = 2$	$Pr = 3$	$Pr = 1$	$Pr = 2$	$Pr = 3$
0.5	0.955	1.471	1.869	0.95487	1.4713	1.8687
	0.677	1.074	1.381	0.67958	1.0734	1.3806
	0.532	0.863	1.121	0.54038	0.8632	1.1213

3. Results and discussion

In this section, we will show the impacts of sundry parameters on the velocity and temperature.

Table 2: Values of $|C_f|$ for various values of the parameters at $Re = 1$

λ	M	Da	$ C_f $
.0	0	0	0.906392
.2	0	0	1.17199
.4	0	0	1.42792
.4	0.5	0	1.83867
.4	1	0	2.16988
.4	1	0.5	2.4544
.4	1	1	2.70492

3.1. Velocity field

The impacts of the pertinent parameters on the fluid velocity are shown in Figs. 2-4. Fig. 2 shows the impact of the viscoelastic parameter λ on the velocity. Fig. 2 shows that an increase in the viscoelastic parameter leads to an increase in the velocity. Fig. 3 exhibits the variation of velocity distribution for various values of the magnetic parameter M . It is observed that an elevation of the magnetic parameter will decrease the velocity within the boundary layer because the impedance force will diminish the fluid velocity. Physically, high values of M increase the Lorentz forces that act as friction against fluid flow, which reduces the thickness of the momentum boundary layer and reduces the velocity. The effect of the porous parameter Da on the velocity is shown in Fig. 4. It is noticed that an increase in the porous parameter decelerates the velocity due to increased obstruction in porous media. This is due to a decrease in the resistance of the porous medium, which causes an increase in the thickness of the momentum boundary layer.

3.2. Fluid temperature

The behavior of fluid temperature ϑ through the boundary layer for sundry values of the parameters of interest is demonstrated graphically through Figs. 5-8. Fig. 5 depicts the variations of temperature

distribution for different values of the viscoelastic parameter λ . As expected, the increase in the viscoelastic parameter accelerated the motion in a boundary layer, which in turn is responsible for reducing the temperature in a boundary layer. The elevation of the magnetic parameter M enhances the fluid temperature in the thermal boundary layer, as shown in Fig. 6. Fig. 7 is prepared to show the effect of the porous parameter Da on the fluid temperature. Fig. 7 reveals that the temperature profile increases by increasing Da . The thickness of the temperature boundary layer increases by increasing the radiation parameter β as depicted in Fig. 8. Physically, a high value of β indicates that the mean absorption coefficient has decreased, which raises the surface heat flow and causes the temperature profile to rise.

4. Conclusions

The present work investigated the problem of the boundary layer flow and heat transfer of the MHD second-grade fluid due to an exponential stretching sheet. By utilizing similarity transformations, the governing equations are transformed into a set of non-linear ordinary differential equations. The system of non-linear ordinary differential equations has been solved via the homotopy analysis method (HAM). The results of this study are shown in the form of graphs and tables. The conclusion may be summed up as follows:

- Our results are in very good agreement compared with the numerical results obtained by Bidin and Nazar (2009).
- A higher value of β indicates that the mean absorption coefficient has decreased, which raises the surface heat flow and causes the temperature profile to rise.
- We concluded that the skin friction coefficient increases by increasing the viscoelastic, magnetic, and porous parameters.

- It is noticed that an increase in the viscoelastic parameter leads to an increase in fluid velocity and reduces the temperature in a boundary layer.
- The thickness of the temperature boundary layer increases by increasing the radiation parameter.

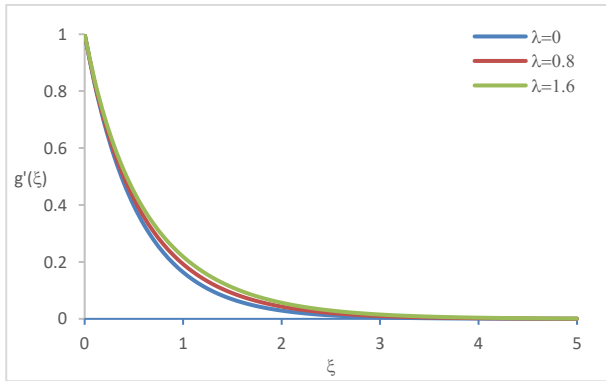


Fig. 2: The velocity versus ξ for different values of the viscoelastic parameter λ

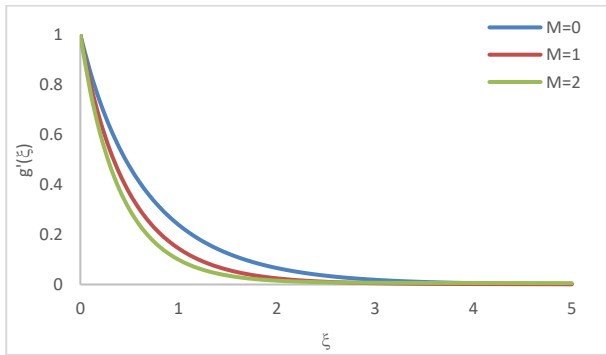


Fig. 3: The velocity versus ξ for different values of the magnetic parameter M

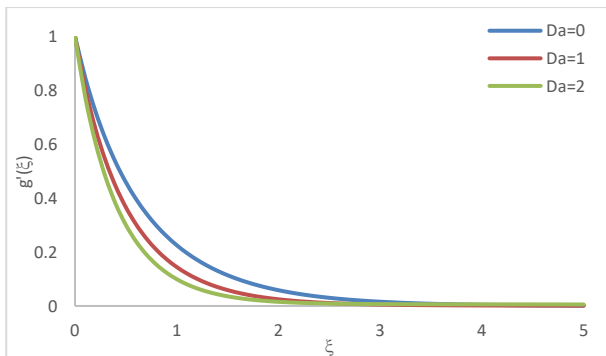


Fig. 4: The velocity versus ξ for different values of the porous parameter Da

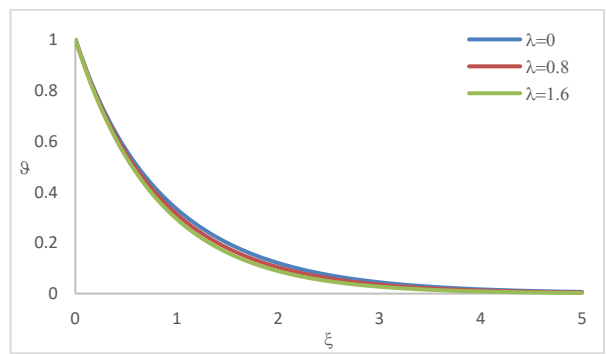


Fig. 5: The temperature versus ξ for different values of the viscoelastic parameter λ

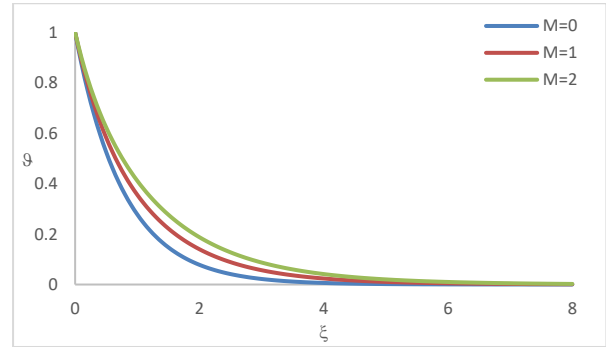


Fig. 6: The temperature versus ξ for different values of the magnetic parameter M

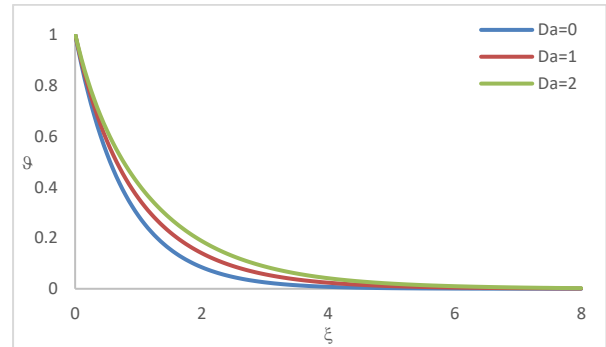


Fig. 7: The temperature versus ξ for different values of the porous parameter Da

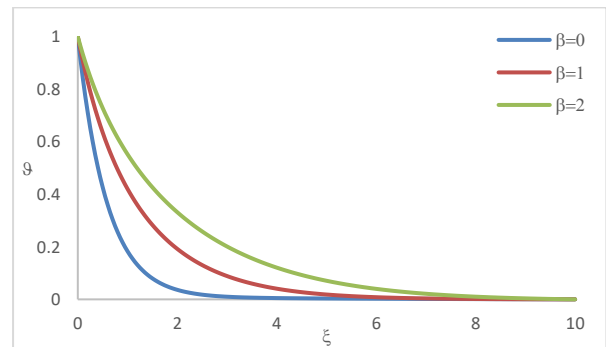


Fig. 8: The temperature versus ξ for different values of the radiation parameter β

List of symbols

(X, Y)	Cartesian coordinates [m]
(U, V)	Velocity components [ms^{-1}]
ν	Kinematic viscosity [m^2s^{-1}]
q	The heat flux
k	Thermal conductivity
T	Fluid Temperature [K]
α	Thermal diffusivity [m^2s^{-1}]
ρc	Fluid capacity heat [$\text{J m}^{-3} \text{K}^{-1}$]
C_p	Specific heat [J/kg K]
D	Diffusion coefficient
L	Reference length [m]
A	temperature exponent
Pr	Prandtl number
U_w	Velocity at the wall [ms^{-1}]
T_w	Surface temperature [K]
γ	Viscoelastic parameter
β	The radiation parameter
σ	Electrical conductivity
λ	The viscoelastic parameter
Da	The porous parameter
M	Magnetic parameter
ξ	Similarity variable

g	Dimensionless velocity
ϑ	Dimensionless temperature

Compliance with ethical standards

Conflict of interest

The author(s) declared no potential conflicts of interest with respect to the research, authorship, and/or publication of this article.

References

- Bidin B and Nazar R (2009). Numerical solution of the boundary layer flow over an exponentially stretching sheet with thermal radiation. *European Journal of Scientific Research*, 33(4): 710-717.
- Chhabra RP and Richardson JF (1999). *Non-Newtonian flow in the process industries: fundamentals and engineering applications*. Butterworth-Heinemann, Oxford, UK.
- Daniel YS, Aziz ZA, Ismail Z, and Salah F (2017). Effects of thermal radiation, viscous and Joule heating on electrical MHD nanofluid with double stratification. *Chinese Journal of Physics*, 55(3): 630-651. <https://doi.org/10.1016/j.cjph.2017.04.001>
- Elbashbeshy EMA (2001). Heat transfer over an exponentially stretching continuous surface with suction. *Archives of Mechanics*, 53(6): 643-651.
- Emam TG and Elmaboud YA (2017). Three-dimensional magneto-hydrodynamic flow over an exponentially stretching surface. *International Journal of Heat and Technology*, 35(4): 987-996. <https://doi.org/10.18280/ijht.350435>
- Hayat T, Javed T, and Abbas Z (2008). Slip flow and heat transfer of a second grade fluid past a stretching sheet through a porous space. *International Journal of Heat and Mass Transfer*, 51(17-18): 4528-4534. <https://doi.org/10.1016/j.ijheatmasstransfer.2007.12.022>
- Hsieh JC, Chen TS, and Armaly BF (1993). Nonsimilarity solutions for mixed convection from vertical surfaces in porous media: Variable surface temperature or heat flux. *International Journal of Heat and Mass Transfer*, 36(6): 1485-1493. [https://doi.org/10.1016/S0017-9310\(05\)80059-6](https://doi.org/10.1016/S0017-9310(05)80059-6)
- Kalpana G, Madhura KR, and Kudenatti RB (2022). Numerical study on the combined effects of Brownian motion and thermophoresis on an unsteady magnetohydrodynamics nanofluid boundary layer flow. *Mathematics and Computers in Simulation*, 200: 78-96. <https://doi.org/10.1016/j.matcom.2022.04.010>
- Kausar MS, Hussanan A, Waqas M, and Mamat M (2022). Boundary layer flow of micropolar nanofluid towards a permeable stretching sheet in the presence of porous medium with thermal radiation and viscous dissipation. *Chinese Journal of Physics*, 78: 435-452. <https://doi.org/10.1016/j.cjph.2022.06.027>
- Kefayati GR (2016). Simulation of heat transfer and entropy generation of MHD natural convection of non-Newtonian nanofluid in an enclosure. *International Journal of Heat and Mass Transfer*, 92: 1066-1089. <https://doi.org/10.1016/j.ijheatmasstransfer.2015.09.078>
- Khan Z, ul Haq S, Ali F, and Andualet M (2022). Free convection flow of second grade dusty fluid between two parallel plates using Fick's and Fourier's laws: A fractional model. *Scientific Reports*, 12: 3448. <https://doi.org/10.1038/s41598-022-06153-3>
PMid:35236870 PMCID:PMC8891311
- Khashi'ie NS, Arifin NM, and Pop I (2022). Magnetohydrodynamics (MHD) boundary layer flow of hybrid nanofluid over a moving plate with Joule heating. *Alexandria Engineering Journal*, 61(3): 1938-1945. <https://doi.org/10.1016/j.aej.2021.07.032>
- Liu CJ, Wang D, Xie F, and Yang T (2020). Magnetic effects on the solvability of 2D MHD boundary layer equations without resistivity in Sobolev spaces. *Journal of Functional Analysis*, 279(7): 108637. <https://doi.org/10.1016/j.jfa.2020.108637>
- Magyari E and Keller B (1999). Heat and mass transfer in the boundary layers on an exponentially stretching continuous surface. *Journal of Physics D: Applied Physics*, 32: 577. <https://doi.org/10.1088/0022-3727/32/5/012>
- Nakayama A and Koyama H (1987). Effect of thermal stratification on free convection within a porous medium. *Journal of Thermophysics and Heat Transfer*, 1(3): 282-285. <https://doi.org/10.2514/3.40>
- Pal D (2010). Magnetohydrodynamic non-Darcy mixed convection heat transfer from a vertical heated plate embedded in a porous medium with variable porosity. *Communications in Nonlinear Science and Numerical Simulation*, 15(12): 3974-3987. <https://doi.org/10.1016/j.cnsns.2010.02.003>
- Reddy BP, Makinde OD, and Hugo A (2022). A computational study on diffusion-thermo and rotation effects on heat generated mixed convection flow of MHD Casson fluid past an oscillating porous plate. *International Communications in Heat and Mass Transfer*, 138: 106389. <https://doi.org/10.1016/j.icheatmasstransfer.2022.106389>
- Roy NC and Pop I (2020). Flow and heat transfer of a second-grade hybrid nanofluid over a permeable stretching/shrinking sheet. *The European Physical Journal Plus*, 135: 768. <https://doi.org/10.1140/epjp/s13360-020-00788-9>
- Shah NA, Yook SJ, and Tosin O (2022). Analytic simulation of thermophoretic second-grade fluid flow past a vertical surface with variable fluid characteristics and convective heating. *Scientific Reports*, 12: 5445. <https://doi.org/10.1038/s41598-022-09301-x>
PMid:35361813 PMCID:PMC8971449
- Sheikholeslami M (2018). Magnetic source impact on nanofluid heat transfer using CVFEM. *Neural Computing and Applications*, 30: 1055-1064. <https://doi.org/10.1007/s00521-016-2740-7>
- Sheikholeslami M (2019a). New computational approach for exergy and entropy analysis of nanofluid under the impact of Lorentz force through a porous media. *Computer Methods in Applied Mechanics and Engineering*, 344: 319-333. <https://doi.org/10.1016/j.cma.2018.09.044>
- Sheikholeslami M (2019b). Numerical approach for MHD Al₂O₃-water nanofluid transportation inside a permeable medium using innovative computer method. *Computer Methods in Applied Mechanics and Engineering*, 344: 306-318. <https://doi.org/10.1016/j.cma.2018.09.042>
- Trüesdell C and Noll W (1965). The nonlinear field theories of mechanics, *Handbuch der Physics V1*. Springer-Verlag, Berlin, Germany. https://doi.org/10.1007/978-3-642-46015-9_1
- Urgorri FR, Moreno C, Fernández-Berceruelo I, and Rapisarda D (2021). The influence of MHD boundary layers on tritium permeation in PbLi flows for fusion breeding blankets. *International Journal of Heat and Mass Transfer*, 181: 121906. <https://doi.org/10.1016/j.ijheatmasstransfer.2021.121906>
- Vajravelu K and Roper T (1999). Flow and heat transfer in a second-grade fluid over a stretching sheet. *International Journal of Non-Linear Mechanics*, 34(6): 1031-1036. [https://doi.org/10.1016/S0020-7462\(98\)00073-0](https://doi.org/10.1016/S0020-7462(98)00073-0)
- Zainal NA, Nazar R, Naganthran K, and Pop I (2021). MHD flow and heat transfer of hybrid nanofluid over a permeable moving surface in the presence of thermal radiation. *International Journal of Numerical Methods for Heat and Fluid Flow*, 31(3): 858-879. <https://doi.org/10.1108/HFF-03-2020-0126>